Pis'ma v ZhETF, vol. 97, iss. 5, pp. 287 – 290 © 2013 March 10

Tunable hybrid surface waves supported by a graphene layer

I. V. Iorsh[+1)], *I. V. Shadrivov*[*], *P. A. Belov*[+], *Yu. S. Kivshar*[+*]

[+]*St.-Petersburg National Research University of Information Technologies, Mechanics and Optics, 197101 St.-Petersburg, Russia*

[*]*Nonlinear Physics Center, Research School of Physics and Engineering, Australian National University, 0200 Canberra ACT, Australia*

Submitted 4 December 2012

We study electromagnetic waves localized near a surface of a semi-infinite dielectric medium covered by a layer of graphene in the presence of a strong external magnetic field. We demonstrate that a novel type of hybrid TE–TM polarized surface plasmons can propagate along the graphene layer. We analyze the effect of the Hall conductivity on the polarization properties of these hybrid surface waves and suggest a possibility to tune the graphene plasmons by the external magnetic field.

DOI: 10.7868/S0370274X13050020

Graphene, two-dimensional lattice of carbon atoms, exhibits a wide range of unique electronic and optical properties [1–3]. It was shown theoretically [4–8] and demonstrated experimentally [9, 10] that a specific type of localized waves, surface plasmon polaritons, can propagate along a single layer of graphene or its bilayer. It was shown that both TM and TE polarized plasmons can exist in graphene [11], and their dispersion properties can be changed by applying an external gate voltage to the graphene sheet which allows to construct effective two-dimensional metamaterial structures based on grapheme [12–15].

One of the key features of graphene is the linear dispersion of the electrons close to the band-edges which is similar to the dispersion of ultra-relativistic Dirac fermions [1–3]. In particular, this leads to the square-root dependence of the electron cyclotron frequency on the magnetic field, and much larger separation of the Landau levels in graphene, and consequently to the possibility to observe quantum Hall effect at room temperatures [16].

In this Letter, we study the properties of electromagnetic waves localized near a surface of a semi-infinite dielectric medium covered by a layer of graphene in the presence of a strong external magnetic field. We demonstrate that the polarization properties of the surface waves supported by a graphene layer can be tuned by varying the value of the magnetic field.

We consider a simple geometry depicted schematically in Fig. 1, where a sheet of graphene is placed at an interface separating two dielectric media. The graphene layer is treated as a conductive surface [11] defined

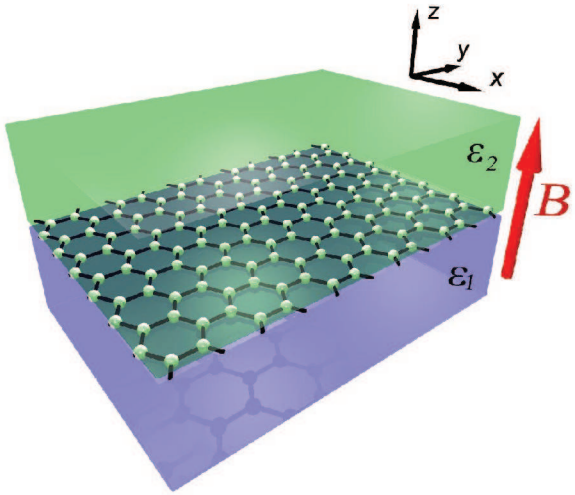

Fig. 1. Geometry of the structure under consideration. A layer of graphene is placed at the interface of two dielectric media (in our case, the upper medium is air). External magnetic field is applied along the z-axis

by frequency-dependent conductivity $\sigma_0(\omega)$. When we apply a constant magnetic field perpendicular to the graphene sheet the conductivity becomes a tensor with the components written as

$$\hat{\sigma} = \begin{pmatrix} \sigma_0 & \sigma_H \\ -\sigma_H & \sigma_0 \end{pmatrix}, \qquad (1)$$

where σ_0 and σ_H are the longitudinal and Hall components of conductivity, respectively. Boundary conditions for the tangential components of the electric and magnetic fields can be written in the form

$$(\mathbf{E}_2 - \mathbf{E}_1) \times \hat{z} = 0, \quad (\mathbf{H}_2 - \mathbf{H}_1) \times \hat{z} = \frac{4\pi}{c}\hat{\sigma}\mathbf{E}_{\|}. \qquad (2)$$

[1)]e-mail: i.iorsh@phoi.ifmo.ru

For both the media, we look for the surface waves with harmonic temporal dependence $\exp(-i\omega t)$ and with the spatial variation corresponding to surface waves decaying inside of the dielectric media, $\mathbf{E}_{1,2}, \mathbf{H}_{1,2} \sim \exp(i\beta x \pm \pm \kappa_{1,2} z)$, where $\kappa_{1,2} = (\beta^2 - \varepsilon_{1,2} k_0^2)^{1/2}$.

The waves in both the media can be presented as a linear combination of the TE and TM polarized waves, so that for the TM polarized waves we have:

$$\mathbf{E}_{1,2}^{\mathrm{TM}} = \left(\mp \frac{i\kappa_{1,2}}{k_0 \varepsilon_{1,2}}, 0, -\frac{\beta}{k_0 \varepsilon_{1,2}} \right),$$

$$\mathbf{H}_{1,2}^{\mathrm{TM}} = (0, 1, 0),$$

whereas for the TE polarized waves, we have

$$\mathbf{H}_{1,2}^{\mathrm{TE}} = \left(\pm \frac{i\kappa_{1,2}}{k_0}, 0, \frac{\beta}{k_0} \right),$$

$$\mathbf{E}_{1,2}^{\mathrm{TE}} = (0, 1, 0).$$

Next, we consider linear combinations of TE and TM polarized waves in both the media, and write the electric fields in the form: $\mathbf{E}_{1,2} = \mathcal{A}\mathbf{E}_{1,2}^{\mathrm{TM}} + \mathcal{B}\mathbf{E}_{1,2}^{\mathrm{TE}}$. To match the waves at two different half-space spaces, we apply the continuity boundary conditions and derive the resulting equations for the amplitudes $\mathcal{A}$ and $\mathcal{B}$,

$$-\frac{4\pi\sigma_{\mathrm{H}}\kappa_1}{ck_0\varepsilon_1}\mathcal{A} + \left(\frac{4\pi i\sigma_0}{c} - \frac{\kappa_2 + \kappa_1}{k_0} \right) \mathcal{B} = 0, \qquad (3)$$

$$\left(\frac{4\pi i\sigma_0\kappa_1}{ck_0\varepsilon_1} + 1 + \frac{\kappa_1\varepsilon_2}{\kappa_2\varepsilon_1} \right) \mathcal{A} - \frac{4\pi\sigma_{\mathrm{H}}}{c}\mathcal{B} = 0, \qquad (4)$$

which allow to obtain the dispersion relations for the surface waves by setting the determinant of the system to zero,

$$\left(\frac{i\sigma_0}{c} - \frac{\kappa_1 + \kappa_2}{4\pi k_0} \right) \left(\frac{i\sigma_0}{c} + \frac{k_0\varepsilon_1}{4\pi\kappa_1} + \frac{k_0\varepsilon_2}{4\pi\kappa_2} \right) = \frac{4\pi}{c^2}\sigma_{\mathrm{H}}^2. \qquad (5)$$

The dispersion relation is in agreement with recent results presented in Ref. [17]. When $\sigma_{\mathrm{H}} = 0$, there exist two solutions corresponding to the dispersion of independent TE and TM polarized surface waves propagating in a graphene layer. However, when $\sigma_{\mathrm{H}} \neq 0$ two polarizations become coupled, and surface waves acquire a hybrid TE–TM polarized structure. The Hall conductivity σ_{H} plays a role of the coupling parameter.

The general expressions for the longitudinal and Hall conductivities can be obtained using the Kubo formula [18, 19],

$$\sigma_0(\omega) = \frac{e^2 v_{\mathrm{F}}^2 |eB|(\hbar\omega + 2i\Gamma)}{\pi c i} \times \sum_{n=0}^{\infty} \qquad (6)$$

$$\left\{ \frac{[n_{\mathrm{F}}(M_n) - n_{\mathrm{F}}(M_{n+1})] - [n_{\mathrm{F}}(-M_n) - n_{\mathrm{F}}(-M_{n+1})]}{(M_{n+1} - M_n)^3 - (\hbar\omega + 2i\Gamma)^2 (M_{n+1} - M_n)} + \right.$$

$$\left. \frac{[n_{\mathrm{F}}(-M_n) - n_{\mathrm{F}}(M_{n+1})] - [n_{\mathrm{F}}(M_n) - n_{\mathrm{F}}(-M_{n+1})]}{(M_{n+1} + M_n)^3 - (\hbar\omega + 2i\Gamma)^2 (M_{n+1} + M_n)} \right\},$$

$$\sigma_{\mathrm{H}}(\omega) = -\frac{e^2 v_{\mathrm{F}}^2 eB}{\pi c} \times \sum_{n=0}^{\infty} \qquad (7)$$

$$\{[n_{\mathrm{F}}(M_n) - n_{\mathrm{F}}(M_{n+1})] + [n_{\mathrm{F}}(-M_n) - n_{\mathrm{F}}(-M_{n+1})]\} \times$$

$$\frac{2[M_n^2 + M_{n+1}^2 - (\hbar\omega + 2i\Gamma)^2]}{[M_n^2 + M_{n+1}^2 - (\hbar\omega + 2i\Gamma)^2]^2 - 4M_n^2 M_{n+1}^2},$$

where M_n is the energy of the corresponding Landau level, $M_n = v_{\mathrm{F}} (2\hbar eB/c)^{1/2}$, n_{F} is the Fermi–Dirac distribution function, v_{F} is the Fermi velocity of the electrons in graphene, and Γ is the electron scattering rate. For the numerical studies of the surface wave dispersion, we use the chemical potential $\mu = 44$ meV and temperature $T = 10$ K. Electron scattering rate Γ is chosen to be 1.3 meV which is in agreement with experimental results [20]. In this case Fermi energy lies between the zero and the first Landau levels. We consider the frequency range from 2 to 300 meV. There exist three allowed transitions between the Landau levels in this frequency range which are depicted in Fig. 2a.

Transition from zero to the first Landau level corresponds to low-frequency resonance in longitudinal and Hall conductivities (see Figs. 2b, c). Transitions from the -2nd to the 1st and from the -1st to the 2nd Landau levels have the same frequency and correspond to the high frequency resonance in conductivity dispersions. Dispersion of the longitudinal and Hall conductivities is shown in Figs. 2b, c. Resonances in the dispersion of conductivities associated with the transitions between the corresponding Landau levels can be controlled with the magnetic field.

To demonstrate the importance of the Hall conductivity in the presence of an external magnetic field, we compare the obtained dispersion relations with the case where we only account for the longitudinal part of the conductivity. Numerical calculations are performed for the values of $\varepsilon_1 = 4$ and $\varepsilon_2 = 1$. Dispersion of the real and imaginary parts of the waveguide number β are presented in Figs. 2d, e.

When the magnetic field is absent, only one surface wave can exist for each frequency: the TE-like polar-

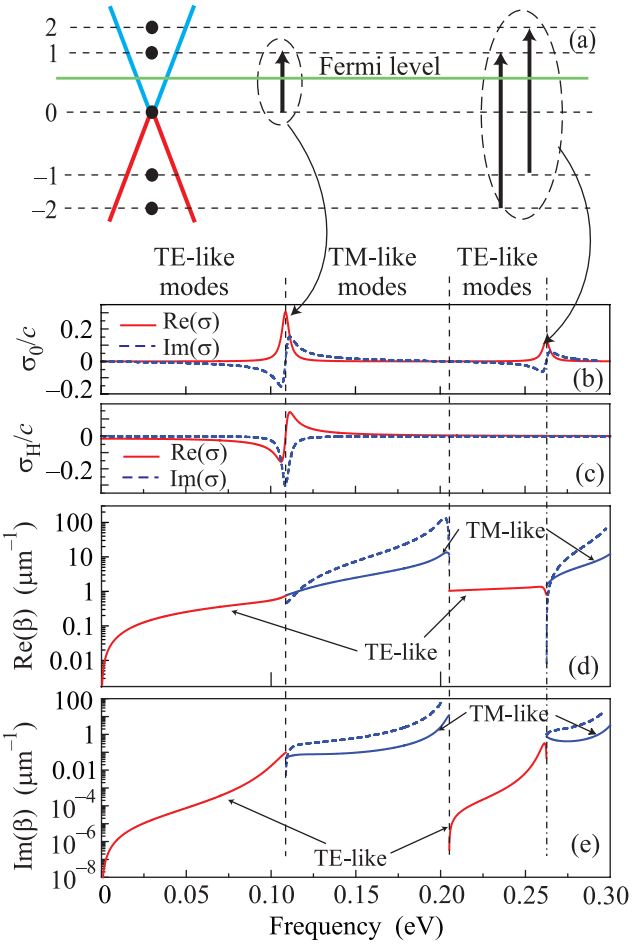

Fig. 2. (a) – First three low-energy transitions of the Landau levels in graphene. (b, c) – Spectrum of the conductivities: red lines correspond to real part, blue lines – to imaginary part. (d) – Dispersion of the real part of the waveguide number of the surface states. (e) – Dispersion of the imaginary part of the waveguide number. Solid red lines correspond to TE-like modes, solid blue to TM-like modes; dashed blue lines correspond to dispersion of TM-like modes without accounting for the Hall conductivity

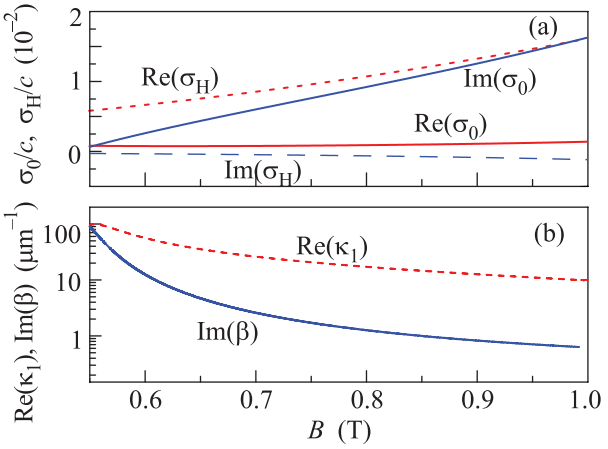

Fig. 3. (Color online) (a) – Dependence of the longitudinal and Hall conductivity of a graphene layer on the external magnetic field; the frequency is 0.19 eV. Red lines correspond to the real part of conductivity, blue – to the imaginary part; solid lines correspond to the longitudinal conductivity, dashed – to Hall conductivity. (b) – Dependence of the inverse propagation length (solid blue line) and inverse localization length (red dashed line) on the external magnetic field

ized mode, for the case when $\mathrm{Im}(\sigma_0) < 0$, and TM-like polarized mode, for the case when $\mathrm{Im}(\sigma_0) > 0$. Hall conductivity significantly changes the real and imaginary parts of wavenumbers [17] and the corresponding properties of surface waves, so that the surface waves become hybrid with mixed TE and TM polarizations.

Dependence of the surface-wave dispersion on the external magnetic field suggests a new degree of freedom for tuning the surface modes in graphene. To illustrate this property, in Fig. 3 we plot the dependence of the wavenumber on the value of the external magnetic field at the fixed frequency $\omega = 0.19\,\mathrm{eV}$. As shown in Fig. 3b, changing the magnetic field from 0.5 to 1 Tesla we can change the localization length of the surface waves, which is inversely proportional to $\mathrm{Re}(\kappa_1)$, and the propagation distance, which is inversely proportional to $\mathrm{Im}(\beta)$, by at least two orders of magnitude.

Furthermore, since the eigenmodes of the graphene sheet in the presence of external magnetic field are hybrid TE–TM modes, we can expect that the we can tune the polarization degree of the surface mode with the external magnetic field. In order to study the polarization of the surface mode we introduce the Stokes parameters S_1, S_2, and S_3 normalized to the full electric field intensity $S_0 = I = |E_x|^2 + |E_y|^2$,

$$S_1 = \frac{|E_x|^2 - |E_y|^2}{|E_x|^2 + |E_y|^2}, \quad S_2 = \frac{2\mathrm{Re}(E_x E_y^*)}{|E_x|^2 + |E_y|^2},$$

$$S_3 = \frac{\mathrm{Re}(E_x E_y^*)}{|E_x|^2 + |E_y|^2}.$$

Parameters S_1 and S_2 describe the state of linear polarization, while parameter S_3 is non-zero for elliptical polarization. Since the Stokes parameters are normalized, then

$$S_1^2 + S_2^2 + S_3^2 = 1.$$

Figure 4b shows the dependence of the Stokes parameters of the surface mode on the external magnetic field. We observe that in the region where the surface mode is TM-like (positive imaginary part of the longitudinal conductivity), the mode is almost fully linearly

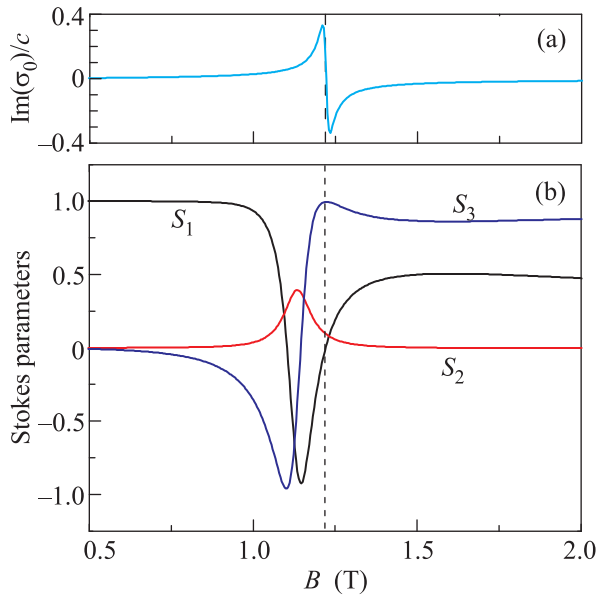

Fig. 4. (a) – Dependence of the imaginary part of longitudinal conductivity of a graphene layer on the external magnetic field; the frequency is 0.19 eV. (b) – Dependence of the Stokes parameters on the external magnetic field

polarized, with vanishing electric field component E_y. However, as we approach the Landau level transition resonance, the mode becomes more circularly polarized. It is noteworthy, that in a small region close to the resonance, the mode changes from counter-clockwise rotation to the clock-wise rotation, which can be seen in a sharp change of the parameter S_3 from -1 to 1 at the point, where the imaginary part of conductivity changes its sign. It can be also seen, that when the mode becomes TE-like for larger magnetic fields, the circular polarization degree remains quite significant at about 0.9, with only small contribution from the linear polarization. This is common feature for all TE-like surface modes in this structure – they are essentially circularly polarized modes, whereas the TM-like modes are rather linearly polarized.

In conclusion, we have demonstrated that, by applying an external magnetic field to a single graphene layer deposited on a dielectric substrate can significantly modify the optical properties of its plasmonic modes. We have shown that in the presence of magnetic field surface hybrid TE–TM polarized plasmons can propagate along the graphene-covered surface, and that the polarization of these surface waves can be controlled by changing the value of the external magnetic field.

This work was supported by the Ministry of Education and Science of Russian Federation, the Dynasty Foundation, and the Australian Research Council.

1. R. R. Nair, P. Blake, A. N. Grigorenko et al., Science **320**, 1308 (2008).
2. F. Bonaccorso, Z. Sun, T. Hasan, and A. C. Ferrari, Nat. Photon. **4**, 611 (2010).
3. Q. Bao and K.P. Loh, ACS Nano **6**, 3677 (2012).
4. Y. V. Bludov, M. I. Vasilevskiy, and N. M. R. Peres, EPL **92**, 608001 (2010).
5. F. H. L. Koppens, D. E. Chang, and F. J. G. de Abajo, Nano Lett. **11**, 3370 (2011).
6. M. Jablan, H. Buljan, and M. Soljacic, Opt. Express **19**, 11236 (2011).
7. A. Y. Nikitin, F. Guinea, F. J. Garcia-Vidal, and L. Martin-Moreno, Phys. Rev. B **84**, 195446 (2011).
8. B. E. Sernelius, Phys. Rev. B **85**, 195427 (2012).
9. Z. Fei, A. S. Rodin, G. O. Andreev et al., Nature **487**, 82 (2012).
10. J. Chen, M. Badioli, P. Alonso-Gonzales et al., Nature **487**, 77 (2012).
11. S. A. Mikhailov and K. Ziegler, Phys. Rev. Lett. **99** 016803, (2007).
12. A. Vakil and N. Engheta, Science **332**, 1291 (2011).
13. L. Ju, B. Geng, J. Horng et al., Nature Nanotechnology, **6**, 630 (2011).
14. S. H. Lee, M. Choi, T. Kim et al., Nature Materials, **11**, 936 (2012).
15. P. Tassin, T. Koschny, M. Kafesaki, and C. M. Soukoulis, Nature Photonics **6**, 259 (2012)
16. K. S. Novoselov, Z. Jiang, Y. Zhang et al., Science **315**, 1379 (2007).
17. A. Ferreira, N. M. R. Peres, and A. H. Castro-Neto, Phys. Rev. B **85**, 205426 (2012).
18. V. P. Gusynin, S. G. Sharapov, and J. P. Carbotte, J. Phys. Cond. Mat. **19**, 026222 (2007).
19. T. Stauber, N. M. R. Peres, and A. K. Geim, Phys. Rev. B **78**, 085432 (2008).
20. Z. Q. Li, E. A. Henriksen, Z. Jiang et al., Nat. Phys. **4**, 532 (2008).